A Novel Model for Breast Cancer Detection and Classification

Nishant Behar
Department of Computer Science & Engineering
Guru Ghasidas University
Bilaspur, India
nishant.itggv@gmail.com

Manish Shrivastava
Department of Computer Science & Engineering
Guru Ghasidas University
Bilaspur, India
manbsp@gmail.com

Received: 2 June 2022 | Revised: 9 September 2022 | Accepted: 12 September 2022

Abstract-Breast cancer is a dreadful disease that affects women globally. The occurrences of masses in the breast region are the main cause of breast cancer development. It is important to detect breast cancer as early as possible as this might increase survival rate. The existing research methodologies have the problems of increased computation complexity and low detection accuracy. To overcome such problems, this paper proposes an efficient breast cancer detection and classification system based on mammogram images. Initially, the mammogram images are preprocessed so unwanted regions and noise are removed and the contrast of the images is enhanced using Homo Morphic Adaptive Histogram Equalization (HMAHE). Then, the breast boundaries are identified with the use of the canny edge detector. After that, the pectoral muscles present in the images are detected and removed using the Global Pixel Intensity-based Thresholding (GPIT) method. Then, the tumors are identified and segmented by the Centroid-based Region Growing Segmentation (CRGS) algorithm. Next, the tumors are segmented and clustered and feature extraction is carried out from the clustered tumors. After that, the necessary features are selected by using the Chaotic Function-based Black Widow Optimization Algorithm (CBWOA). The selected features are utilized by the Convolutional Squared Deviation Neural Network Classifier (CSDNN) which classifies the tumors into six different categories. The proposed model effectively detects and classifies breast tumors and its efficiency is experimentally proved by comparison with the existing techniques.

Keywords-classification; feature selection; Chaotic Function-based Black Widow Optimization Algorithm (CBWOA); Convolutional Squared Deviation Neural Network (CSDNN) classifier

I. INTRODUCTION

Cancer is one of the most challenging and fatal diseases worldwide. It is responsible for the loss of millions of lives every year [1]. The instances of growth of Breast Cancer (BC) amongst women in the age group of 30-40 years have increased significantly over the last few decades in India [2]. BC is one of the most frequent cancers in developed and developing countries [3]. BC starts when malignant lumps begin to grow from the breast cells [4]. Globally, BC is the second most common type of cancer and a major cause of human morbidity and mortality, disproportionately affecting women [5, 6]. However, according to [7], more than 30% of cancer cases will survive in the long term if they accept accurate early detection [7]. Therefore, early detection of BC is crucial for patients' health and treatment. Early detection relies on testing and examining the pre-presentation of any symptoms [8]. Any suspected breast lump or growth should be immediately checked by the appropriate medical professional, in addition to regular screening tests [9]. Mammography BC diagnostic methods include X-rays, CT scans, ultrasound imaging, etc. It is complicated for doctors to diagnose cancer based on mammogram images due to the complexity of premature BC, combined with the low brightness of mammogram images [10]. Thus, enhancing the detection efficiency via the CAD system of deep learning techniques is essential.

II. LITERATURE REVIEW

Authors in [11] developed an effective computer-aided diagnosis system for breast cancer. Feature weighting was employed because it boosted the classification performance more than feature subset selection. The results showed that the proposed wrapper method had a better ability to attain higher accuracy as compared to the existing techniques. The method had low specificity in breast cancer diagnosis. Authors in [12] explored an improved Computer-Aided Diagnosis (CAD) model for the classification of breast masses into the normal or abnormal and benign or malignant categories. It utilized Lifting Wavelet Transform (LWT) to extract the features from the region of interest in mammogram images. Finally, classification was performed using a combination of an extreme learning machine and Moth Flame Optimization (MFO-ELM) technique. The recommended CAD model obtained better performance and also, achieved minimum computational time as compared to other existing models. Authors in [13] proposed Multi-Scale generalized Radial Basis Function (MSRBF) neural networks for image feature extraction, medical image analysis, and classification for breast cancer detection. Initially, the image data were rendered into a Multiple-Input-Single-Output (MISO) system. The Forward Regression Orthogonal Least Squares (FROLS) algorithm was used to solve the system as a model structure detection problem and found the output layer weights. The experimental results showed that the method reached classification accuracy above

Corresponding author: Nishant Behar

93% in the two mammography databases and 86.7% in BreakHis. However, the DCT method needs large processing power. Interested researchers in healthcare can also find interesting research on the automatic detection of breast cancer and biomedical images [14-27].

III. METHODOLOGY

A. The Proposed Model

BC which grows in the breast cells is a malignant tumor, which has the potential of spreading to other body parts. BC infects 2.1 million women every year and is the most common sort of cancer, according to the World Health Organization (WHO). Furthermore, amongst women, the highest number of cancer-associated deaths is associated with BC. In general, the causes for BC are not defined and an exact justification for the occurrence of BC in certain women over others has not been provided yet. Nevertheless, to specify the incidence of BC, there are some common facts about BC symptoms. Most of these symptoms do not appear in the early development stages. Therefore, the process of detecting cancer in its early stage is quite challenging. In order to identify the BC development in the earlier stages itself, a non-invasive methodology termed digital mammography is utilized. DBT along with breast masses or tumors can be seen at increased radiological densities, i.e. they are seen as white, on mammograms. Thus, owing to overlay with DBT, the identification of malignant breast masses becomes a complicated task. Thus, false positives, false negatives, and over-diagnosis are issues which affect mammography. Radiologists are aided with the usage of Artificial Intelligence (AI) via enhanced BCD utilizing mammography. In this paper, ground on the mammogram images, an effectual BCD system has been proposed by utilizing a CSDNN classifier. Analyzing the mammogram images by utilizing CSDNN and mining detection methodologies and classifying the tumor is the main aim of this work. Figure 1 presents the block diagram of the proposed model.

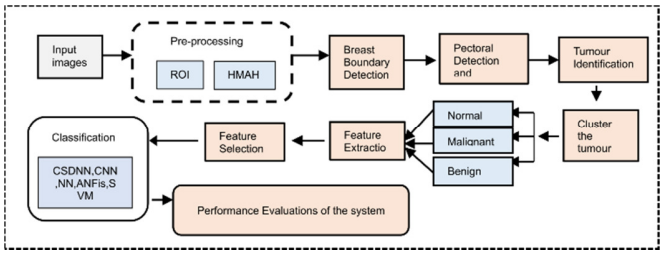

Fig. 1. The general structure of the proposed model for breast cancer classification.

B. Preprocessing

Preprocessing is an important step for removing undesirable noise and irrelevant details and for improving the quality and information content of the original image. The proposed work begins with preprocessing which consists of two steps, i.e. removing unwanted regions and contrast enhancement and noise removal.

Adaptive Histogram Equalization (AHE) is an image processing technique that is used to enhance the contrast of images. AHE divides the image into distinct blocks and computes histogram equalization for each section. Thus, AHE computes many histograms, each corresponding to a distinct section of the image. It enhances the local contrast and definitions of edges in all distinct regions of the image. Hence, in order to improve the performance of the AHE algorithm, in this work, the Homo Morphic (HM) filtering is incorporated with the existing AHE algorithm. Initially, the input images are filtered by the HM filter. HM filtering is commonly used for correcting the non-uniform illumination in images. Moreover, it simultaneously normalizes the brightness across an image and increases contrast.

C. Breast Boundary Detection

After preprocessing, the pre-processed images $R_{pre(m)}$ are applied to Canny Edge Detector, which is a widely used edge detection algorithm to locate sharp intensity changes and find object boundaries in an image. The proposed work utilizes the Canny Edge Detector for detecting breast boundaries. It contains 5 steps called noise reduction, gradient calculations, non-maximum suppression, double threshold, and edge tracking.

D. Pectoral Detection and Removal

The output images from the Canny Edge Detector with the detected breast boundaries $R_{CED(m)}$ are applied to the Global Pixel Intensity-based Thresholding (GPIT) method for removing the pectoral muscles. If the pectoral muscles are present in the images, they may complicate the feature extraction process and result in false classification. To overcome this problem, the pectoral muscles are identified and removed with the GPIT method. The normal thresholding method has the drawback that the selected threshold should correspond to a valley of the histogram. This method does not work well with variable illumination. So, to overcome this drawback, the threshold value is calculated from the pixel intensity of an image. Here, the mean intensity value of all the pixels in the image is used as a global threshold. It can be computed as:

$$\delta_{th} = \frac{1}{N} \sum_{(i,j) \in N} I_{R_{CED(m)}}(i,j) \quad (1)$$

where N is the total number of pixels, $I_{R_{pec\_rem(m)}}(i,j)$ denotes the intensity of the pixel, and δ_{th} denotes the threshold value computed based on the mean value of the pixel intensity value.

E. Tumor Identification

After the pectoral muscles were removed, the images $R_{peec\_rem(m)}$ are inputted to the Centroid-based Region Growing Segmentation (CRGS) algorithm for tumor segmentation in the breast. In general, a tumor occurs when cells divide and grow excessively in the body. Region growing is a simple and efficient approach to segment the objects from an image. The process of region growing is to map the individual pixel to a set of pixels representing distinct image

regions and to grow them until they cover the entire image. The existing region growing algorithm has a limitation, that is, to choose the appropriate seed points and region growing criteria. The random selection of these two factors directly affects the quality of image segmentation. To overcome this limitation, in this paper, the initial seed point is calculated by using the centroid of the maximum area covered by the image. This improvisation drastically increases the segmentation accuracy and overcomes the over and under segmentation issues.

F. Tumor Clustering

After segmentation, the images with the segmented regions $R_{seg(m)}$ are clustered by Divisive Similarity Clustering (DSC). Divisive clustering is a top-down clustering approach, which separates the number of objects successively into finer groupings. The DSC algorithm mostly uses Euclidean distance to calculate the distance between the data points. Although it is a common distance measure, Euclidean distance is not scale invariant which means that the computed distances might be varied and inaccurate. Moreover, the Euclidean distance is not suitable for a large amount of data so that the cosine similarity function is calculated, which provides a better similarity result than the Euclidean distance and achieves better clustering accuracy.

G. Feature Extraction

After clustering, the important features are extracted from the clustered benign L_{Ben} and malignant L_{Mal} regions. Feature extraction helps reducing the amount of redundant data from the data set. In the end, data reduction increases the speed of the learning process. In the proposed work, the important features such as Grey-Level Co-occurrence Matrix (GLCM), shape features, Local Tetra Pattern (LTrP), color intensity, and Gabor features are extracted.

- The GLCM method is a way of extracting second-order statistical texture features. The extracted texture features are autocorrelation, contrast, correlation, cluster shade, dissimilarity, energy, entropy, homogeneity, maximum probability, and difference variance.
- Shape features correspond to the physical structure or the geometric shapes of the objects present in the image.
- LTrP demonstrates the spatial structure of the local texture using the direction of the center pixel. It is the first-order derivative of the center pixel along the 0^o and 90^o directions.
- Gabor features extract local pieces of information which are then combined to recognize an object. From the response of the Gabor filter, the Gabor features are constructed at several orientations and frequencies.
- Color intensity represents the image from a different perspective. It represents the frequency distribution of color bins in an image. It counts similar pixels and stores them. These features extracted from images are then used for image recognition. The extracted features are denoted as:

$$\hbar_n = \{\hbar_1, \hbar_2, \hbar_3, \ldots\ldots\ldots \hbar_N\} \quad (2)$$

where $\hbar_n$ denotes the number of the extracted features.

H. Feature Selection

After feature extraction, the important features are selected using the Chaotic Function-based Black Widow Optimization Algorithm (CBWOA). The BWO algorithm is a meta-heuristic algorithm that delivers fast convergence and avoids local optima. BWO is a good method to solve several types of optimization problems as it keeps the balance between the exploration phase and the exploitation phase. Its fundamental steps and flowchart are given in Figures 2-3. In the proposed model, the optimal features, which enhance the classification accuracy, are selected by utilizing the optimization algorithm.

Input: Extracted feature set $\hbar_n$
Output: Selected features $\hbar_{n(opt)}$

Begin
  Initialize population $\hbar_n$, Cannibalism rate, mutation rate, maximum number of iteration t_{max}
  Evaluate fitness
  Set $t = 1$
  While $(t < \max iter)$
    For $i = 1$ **to** number of reproduction K **//procreate and cannibalism**
      Select the pair of parents using $\hbar_n^{ch}(t+1) = \eta * \hbar_n^{ch}(t) * (1 - \hbar_n^{ch}(t))$
      Generate children using S_1, S_2
      Destroy father and some children based on cannibalism rate
      Evaluate fitness value
      Store best individual
    End for
    Select number of individuals based on the mutation rate
    For $i = 1$ to number of mutations l **//Mutation**
      Select a solution from new population
      Mutate selected individuals
      Evaluate fitness value
      Generate new population
    End for
    Update new population
  End while
  Return the selected features
End

Fig. 2. Pseudo-code of the proposed CBWOA.

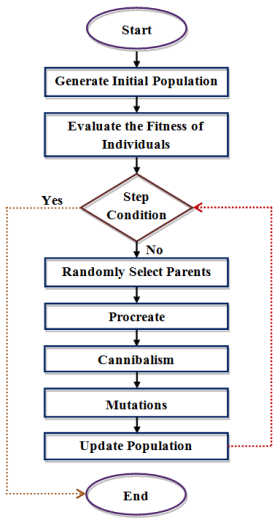

Fig. 3. Flowchart of the proposed CBWOA.

I. CSDNN Classification

The selected optimal features $\hbar_{n(opt)}$ are inputted to the Convolutional CSDNN classifier. A CNN is a multilayer neural

network that contains many hidden layers that perform two important functions, convolution and pooling. Generally, neural networks suffer from the weight initialization problem. In the traditional neural network, the weight value is randomly initialized which causes the classifier to produce a false classification. So, in the proposed classifier, the weight value is initialized based on the mean and variance of its input. The architecture of the proposed CSDNN is shown in Figure 4.

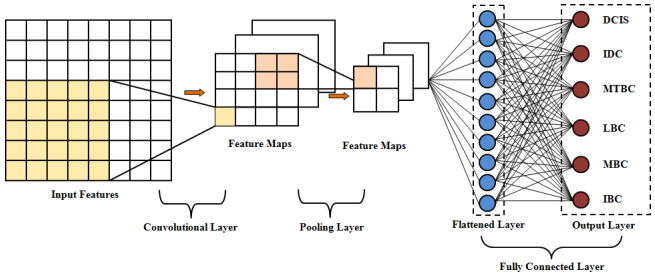

Fig. 4. Architecture of the proposed CSDNN.

1) Convolution Layer

The convolution layer performs the convolution operation between the input features and the weight values (kernels) which is then applied to the non-linear activation layer to return the rectified feature map. The weight updating of CSDNN is done by the mean and variance of the input values. It can be expressed as:

$$\mu_{\hbar_{n(opt)}} = \frac{1}{N}\sum_{n=1}^{N}\hbar_{n(opt)} \quad (3)$$

$$\sigma_{\hbar_{n(opt)}} = \frac{1}{N}\sum_{n=1}^{N}(\hbar_{n(opt)} - \mu_{\hbar_{n(opt)}}) \quad (4)$$

where $\mu_{\hbar_{n(opt)}}$, $\sigma_{\hbar_{n(opt)}}$ are the mean and variance of the input features, and N is the total number of features.

The progress of feature maps in the convolution layer is expressed in (5):

$$L_{Conv}^{fea(n)} = \Omega(\sum \hbar_{n(opt)} * \chi_{wt(\mu_{\hbar_{n(opt)}},\sigma_{\hbar_{n(opt)}})} + \Theta) \quad (5)$$

where $L_{Conv}^{fea(n)}$ denotes the obtained feature map, Ω is the non-linear activation function, $\chi_{wt(\mu_{\hbar_{n(opt)}},\sigma_{\hbar_{n(opt)}})}$ denotes the weight values generated based on the mean and variance of the input, and Θ denotes the bias value for each feature map.

2) Pooling Layer

This layer reduces the size of the input feature map obtained after the convolution. For dimensionality reduction, the max-pooling function is used which detects the most dominating features for faster classification. Thus, the pooled feature map of the pooling layer is expressed as:

$$L_{pool}^{fea(n)} = \Re_{mp}\left(L_{Conv}^{fea(n)}\right) \quad (6)$$

where $L_{pool}^{fea(n)}$ denotes the pooled feature map and $\Re_{mp}(\bullet)$ denotes the max-pooling function.

3) Fully Connected Layer

After a number of convolution and pooling operations, the pooled output is flattened and is applied to the fully connected layer. The fully connected layer feeds the input to the SoftMax layer, which uses the softmax function to convert the input scores into a sum of output probabilities.

IV. EXPERIMENTAL RESULTS

In order to examine the proposed system (Figure 2), numerous experiments were conducted to evaluate the performance of the proposed model and are presented in this section. The proposed breast cancer detection system is developed in the working platform of MATLAB. The dataset description is described in the next section. All chosen samples were first stored into major classes as benign, malignant, and normal classes and subsequently into sub classes.

A. Dataset Description

The performance of the proposed methodology is evaluated by using publicly available data. Sample images have been collected from [28]. The dimension of the input image is 1024×1024 pixels in 'pgm' format. The input mammogram images consist of dense tissue variations, breast density percentage, and breast density variations. These features are helpful to detect breast cancer. Thus, the dataset has 3 main classes: normal, benign (DCIS), malignant and their subclasses.

B. Pre-processing Performance Analysis

In this section, the proposed HMAHE's performance is analogized with the prevailing Histogram Equalization (HE), Contrast Limited Adaptive Histogram Equalization (CLAHE), along with Contrast Stretching (CS) techniques regarding Minimum Squared Error (MSE), Structure Similarity Index Measure (SSIM), Peak Signal to Noise Ratio (PSNR), and Variance Ratio values.

The ratio of the maximum possible power of an image to the power of corrupting noise, which affects the quality of its representation, is named PSNR. The PSNR performance of the proposed and other known methods is analyzed in Figure 5. Good image quality along with fewer errors introduced to the image is attained by achieving a high PSNR value. Accordingly, the PSNR value for the proposed methodology is 61.89734. The PSNR values for CLAHE, HE, and CS frameworks are 58.86085, 58.00242, and 58.37713 respectively, which are lower than that of the proposed technique, proving that the proposed system shows better performance.

C. Segmentation Performance Analysis

By analogizing specificity, accuracy, F-measure, and sensitivity with the outputs of prevailing Active Contour (AC), Watershed (WS), and Region Growing (RG) methodologies, the accuracy of the proposed CRGS segmentation model is determined.

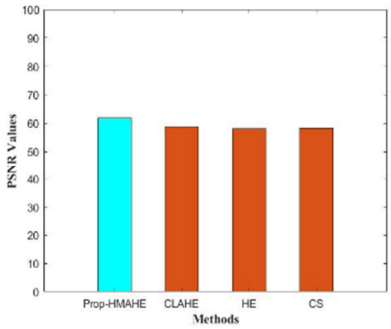

Fig. 5. Performance estimation based on PSNR.

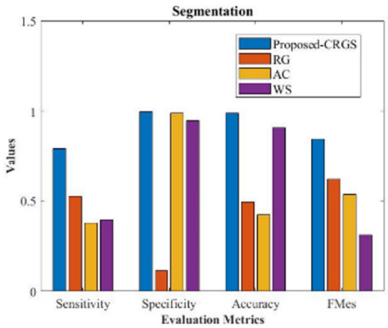

Fig. 6. Performance analysis based on sensitivity, specificity, accuracy, and F-measure.

To estimate the performance of segmentation frameworks utilized to extract objects of interest from images, metrics like specificity, accuracy, F-measure, and sensitivity are important. The proposed and previous segmentation mechanisms' performance in terms of accuracy, F-measure, sensitivity, and specificity is depicted in Figure 6. The sensitivity and specificity values achieved by the proposed technique are 0.794568 and 0.998382. The previous systems have sensitivity and specificity of 0.525349 and 0.113123 for AC, 0.377702 and 0.988604 for RG, and 0.395193 and 0.947311 for WS. The accuracy and F-measure of the proposed system are 0.991286 and 0.846746, which are higher than the existing frameworks'. Therefore, it is concluded that the proposed model segments the objects from the images more effectively.

D. Clustering Performance Analysis

Clustering methods that have high accuracy and time efficiency are more efficient for discovering the required number of clusters. In this sub-section, the performance of the proposed DSC clustering method is evaluated based on the clustering accuracy. For performance evaluation, the proposed method is weighted against the existing Hierarchical Clustering (HC), Fuzzy C-Means (FCM), and K-Means clustering techniques. Table I shows the accuracy of the proposed and existing clustering techniques. The clustering accuracy achieved by the proposed method is 0.961111, whereas the existing methods gave lower accuracy of 0.694444 (HC), 0.544444 (FCM), and 0.627778 (K-Means), indicating that the proposed method has better performance. The graphical representation of the above discussion is shown in Figure 7.

TABLE I. COMPARATIVE ANALYSIS BASED ON CLUSTERING ACCURACY

Methods	Clustering accuracy
Proposed DSC	0.961111
HC	0.694444
FCM	0.544444
KMEANS	0.627778

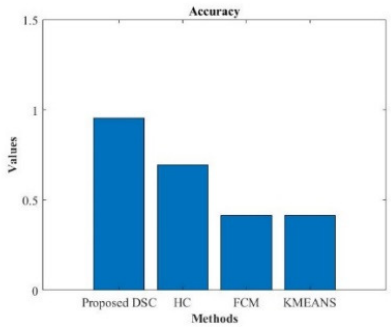

Fig. 7. Performance analysis of the proposed and existing methods based on clustering accuracy.

E. Feature Selection Performance Analysis

The performance of the proposed CBWOA optimization method used for selecting the optimal features was evaluated by comparing the fitness level attained for the number of iterations, and computation time with the existing methods of Genetic Algorithm (GA) and Particle Swarm Optimization (PSO).

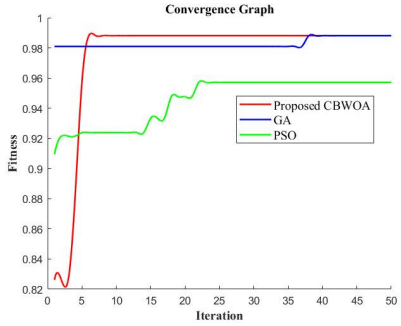

Fig. 8. Fitness vs. Iterations.

The convergence graph of fitness value vs. iteration number is shown in Figure 8. Compared to the existing methods, the fitness value achieved by the proposed method is higher for a varying number of iterations. The proposed method has a 0.957153 fitness value at a minimum of 5 iterations and a 0.988095 fitness value at a maximum of 50 iterations. In the same way, the existing methods have fitness values lower than the proposed method. It is concluded that the proposed method has higher optimal prediction nature than PSO and GA.

F. Classification Performance Analysis

Table II shows the performance of the proposed and existing classifiers with reference to some quality metrics such as sensitivity, specificity, accuracy, and F-measure. Sensitivity delivers the ability to label positive breast cancer cases as positive, whereas specificity indicates the ability to identify

negative breast cancer cases as negative. In order to get an accurate prediction, these values should be high. F-measure is a measure of the model's accuracy, which is calculated by using the precision and recall value.

TABLE II. PERFORMANCE ANALYSIS OF PROPOSED AND EXISTING CLASSIFIERS

Metrics	CSDNN	CNN	NN	ANFIS	SVM
Sensitivity	0.958333	0.325	0.566667	0.808333	0.575
Specificity	0.993056	0.8875	0.927778	0.968056	0.929167
Accuracy	0.988095	0.807143	0.87619	0.945238	0.878571
F-measure	0.958333	0.325	0.566667	0.808333	0.575

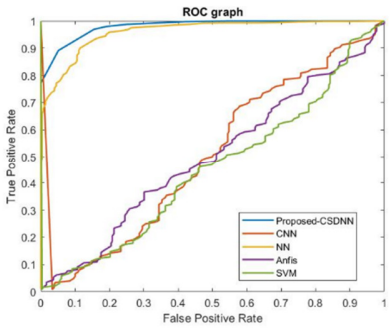

Fig. 9. ROC curve.

The ROC graph for estimating the performance of the proposed and existing classifiers is shown in Figure 9. An overview of true positives and false negatives is provided by the ROC graphs. The better performance is indicated by the classifiers that give curves closer to the top-left corner. The test is less accurate when the curve comes closer to the 45-degree diagonal of the ROC space. Accordingly, we can see that the proposed model is more accurate than the prevailing techniques.

V. DISCUSSION

The proposed method efficiently removes the unwanted regions from breast mammogram images, and outperforms existing works with their inefficient preprocessing functions. The proposed method uses an effective feature selection phase. The main contribution of the feature selection phase is to reduce the complications of the classifier. Thus, the classifier can classify the features with least resource consumption. Most of the existing methodologies have inadequate feature extraction and selection phase [29], drastically reducing their precision level. Furthermore, in the proposed work, a modified classifier is used, in which the optimal weight values are selected by the mean and variance of its input. In most of the existing works, the classifier deals with random weight values [30]. When compared to existing methodologies, the proposed work exhibits better accuracy rates. Moreover, the proposed work classifies the multiple types of breast cancer with less time and cost.

VI. CONCLUSION AND FUTURE WORK

The main goal of the proposed model is to detect breast tumors and classify them according to the type of the detected tumor. In this framework, mammogram images are analyzed and tumors are identified by CRGS methods. If the tumor is found in a mammogram image, then the type of tumor is identified with the CSDNN method. The performance of the proposed CRGS and CSDNN methods were compared with some traditional methods with respect to some evaluation metrics. The experimental results revealed that both CRGS and CSDNN methods achieve greater performance than the existing methods. The proposed CRGS method obtained an accuracy of 0.991286 whereas the proposed CSDNN method attained an accuracy of 0.988095. This performance analysis clearly states that the proposed model accurately detects and classifies breast tumors.

In the future, a more advanced classifier may be integrated to enhance the performance of the proposed model.

REFERENCES

[1] S. Ekici and H. Jawzal, "Breast cancer diagnosis using thermography and convolutional neural networks," *Medical Hypotheses*, vol. 137, Apr. 2020, Art. no. 109542, https://doi.org/10.1016/j.mehy.2019.109542.

[2] D. Singh and A. K. Singh, "Role of image thermography in early breast cancer detection- Past, present and future," *Computer Methods and Programs in Biomedicine*, vol. 183, Jan. 2020, Art. no. 105074, https://doi.org/10.1016/j.cmpb.2019.105074.

[3] M. Abdar and V. Makarenkov, "CWV-BANN-SVM ensemble learning classifier for an accurate diagnosis of breast cancer," *Measurement*, vol. 146, pp. 557–570, Nov. 2019, https://doi.org/10.1016/j.measurement.2019.05.022.

[4] D. A. Omondiagbe, S. Veeramani, and A. S. Sidhu, "Machine Learning Classification Techniques for Breast Cancer Diagnosis," *IOP Conference Series: Materials Science and Engineering*, vol. 495, Jun. 2019, Art. no. 012033, https://doi.org/10.1088/1757-899X/495/1/012033.

[5] P. Jasbi *et al.*, "Breast cancer detection using targeted plasma metabolomics," *Journal of Chromatography B*, vol. 1105, pp. 26–37, Jan. 2019, https://doi.org/10.1016/j.jchromb.2018.11.029.

[6] M. Swellam, R. F. K. Zahran, H. Abo El-Sadat Taha, N. El-Khazragy, and C. Abdel-Malak, "Role of some circulating MiRNAs on breast cancer diagnosis," *Archives of Physiology and Biochemistry*, vol. 125, no. 5, pp. 456–464, Oct. 2019, https://doi.org/10.1080/13813455.2018.1482355.

[7] N. Liu, E.-S. Qi, M. Xu, B. Gao, and G.-Q. Liu, "A novel intelligent classification model for breast cancer diagnosis," *Information Processing & Management*, vol. 56, no. 3, pp. 609–623, May 2019, https://doi.org/10.1016/j.ipm.2018.10.014.

[8] M. M. Rahman, Y. Ghasemi, E. Suley, Y. Zhou, S. Wang, and J. Rogers, "Machine Learning Based Computer Aided Diagnosis of Breast Cancer Utilizing Anthropometric and Clinical Features," *IRBM*, vol. 42, no. 4, pp. 215–226, Aug. 2021, https://doi.org/10.1016/j.irbm.2020.05.005.

[9] Ü. Budak, Z. Cömert, Z. N. Rashid, A. Şengür, and M. Çıbuk, "Computer-aided diagnosis system combining FCN and Bi-LSTM model for efficient breast cancer detection from histopathological images," *Applied Soft Computing*, vol. 85, Dec. 2019, Art. no. 105765, https://doi.org/10.1016/j.asoc.2019.105765.

[10] R. S. Patil and N. Biradar, "Automated mammogram breast cancer detection using the optimized combination of convolutional and recurrent neural network," *Evolutionary Intelligence*, vol. 14, no. 4, pp. 1459–1474, Dec. 2021, https://doi.org/10.1007/s12065-020-00403-x.

[11] S. Dalwinder, S. Birmohan, and K. Manpreet, "Simultaneous feature weighting and parameter determination of Neural Networks using Ant Lion Optimization for the classification of breast cancer," *Biocybernetics and Biomedical Engineering*, vol. 40, no. 1, pp. 337–351, Jan. 2020, https://doi.org/10.1016/j.bbe.2019.12.004.

[12] D. Muduli, R. Dash, and B. Majhi, "Automated breast cancer detection in digital mammograms: A moth flame optimization based ELM

approach," *Biomedical Signal Processing and Control*, vol. 59, May 2020, Art. no. 101912, https://doi.org/10.1016/j.bspc.2020.101912.

[13] C. Beltran-Perez, H.-L. Wei, and A. Rubio-Solis, "Generalized Multiscale RBF Networks and the DCT for Breast Cancer Detection," *International Journal of Automation and Computing*, vol. 17, no. 1, pp. 55–70, Feb. 2020, https://doi.org/10.1007/s11633-019-1210-y.

[14] T. A. Assegie, "An optimized K-Nearest Neighbor based breast cancer detection," *Journal of Robotics and Control (JRC)*, vol. 2, no. 3, 2021, https://doi.org/10.18196/jrc.2363.

[15] H. Dhahri, E. Al Maghayreh, A. Mahmood, W. Elkilani, and M. Faisal Nagi, "Automated Breast Cancer Diagnosis Based on Machine Learning Algorithms," *Journal of Healthcare Engineering*, vol. 2019, pp. 1–11, Nov. 2019, https://doi.org/10.1155/2019/4253641.

[16] H. N. Iqbal, A. B. Nassif, and I. Shahin, "Classifications of Breast Cancer Diagnosis using Machine Learning," *International Journal of Computers*, vol. 14, pp. 86–86, Dec. 2020, https://doi.org/10.46300/9108.2020.14.13.

[17] S. Chaudhury *et al.*, "Effective Image Processing and Segmentation-Based Machine Learning Techniques for Diagnosis of Breast Cancer," *Computational and Mathematical Methods in Medicine*, vol. 2022, pp. 1–6, Apr. 2022, https://doi.org/10.1155/2022/6841334.

[18] R. Chauhan, P. K. Vinod, and C. V. Jawahar, "Exploring Genetic-histologic Relationships in Breast Cancer." arXiv, Mar. 14, 2021, https://doi.org/10.48550/arXiv.2103.08082.

[19] A. Al-Gburi, N. Alwan, E. Al-Tameemi, and W. H.Al-Dabbagh, "Opportunistic Screening for Early Detection of Breast Cancer in Iraq Iraq," *International Medical Journal*, vol. 28, no. 1, pp. 28–32, Feb. 2021.

[20] M. Monirujjaman Khan *et al.*, "Machine Learning Based Comparative Analysis for Breast Cancer Prediction," *Journal of Healthcare Engineering*, vol. 2022, pp. 1–15, Apr. 2022, https://doi.org/10.1155/2022/4365855.

[21] S. Sharma, R. Mehra, and S. Kumar, "Optimised CNN in conjunction with efficient pooling strategy for the multi-classification of breast cancer," *IET Image Processing*, vol. 15, no. 4, pp. 936–946, Mar. 2021, https://doi.org/10.1049/ipr2.12074.

[22] V. Chaurasia, M. Pandey, and S. Pal, "Prediction of Presence of Breast Cancer Disease in the Patient using Machine Learning Algorithms and SFS," *IOP Conference Series: Materials Science and Engineering*, vol. 1099, no. 1, Mar. 2021, Art. no. 012003, https://doi.org/10.1088/1757-899X/1099/1/012003.

[23] J. Quist, L. Taylor, J. Staaf, and A. Grigoriadis, "Random Forest Modelling of High-Dimensional Mixed-Type Data for Breast Cancer Classification," *Cancers*, vol. 13, no. 5, Feb. 2021, Art. no. 991, https://doi.org/10.3390/cancers13050991.

[24] A. B. S. Salamh and H. I. Akyüz, "A Novel Feature Extraction Descriptor for Face Recognition," *Engineering, Technology & Applied Science Research*, vol. 12, no. 1, pp. 8033–8038, Feb. 2022, https://doi.org/10.48084/etasr.4624.

[25] N. Kumar, A. Hashmi, M. Gupta, and A. Kundu, "Automatic Diagnosis of Covid-19 Related Pneumonia from CXR and CT-Scan Images," *Engineering, Technology & Applied Science Research*, vol. 12, no. 1, pp. 7993–7997, Feb. 2022, https://doi.org/10.48084/etasr.4613.

[26] N. K. Al-Shammari *et al.*, "Cardiac Stroke Prediction Framework using Hybrid Optimization Algorithm under DNN," *Engineering, Technology & Applied Science Research*, vol. 11, no. 4, pp. 7436–7441, Aug. 2021, https://doi.org/10.48084/etasr.4277.

[27] A. Kehili, K. Dabbabi, and A. Cherif, "Early Detection of Parkinson's and Alzheimer's Diseases using the VOT_Mean Feature," *Engineering, Technology & Applied Science Research*, vol. 11, no. 2, pp. 6912–6918, Apr. 2021, https://doi.org/10.48084/etasr.4038.

[28] "MIAS Mammography," *Kaggle*. https://www.kaggle.com/datasets/kmader/mias-mammography.

[29] M. Gupta, N. Kumar, N. Gupta, and A. Zaguia, "Fusion of Multi-Modality Biomedical Images Using Deep Neural Networks." Nov. 11, 2021, https://doi.org/10.21203/rs.3.rs-983420/v1.

[30] N. Kumar, N. Narayan Das, D. Gupta, K. Gupta, and J. Bindra, "Efficient Automated Disease Diagnosis Using Machine Learning Models," *Journal of Healthcare Engineering*, vol. 2021, pp. 1–13, May 2021, https://doi.org/10.1155/2021/9983652.